Supplementary Figure S1

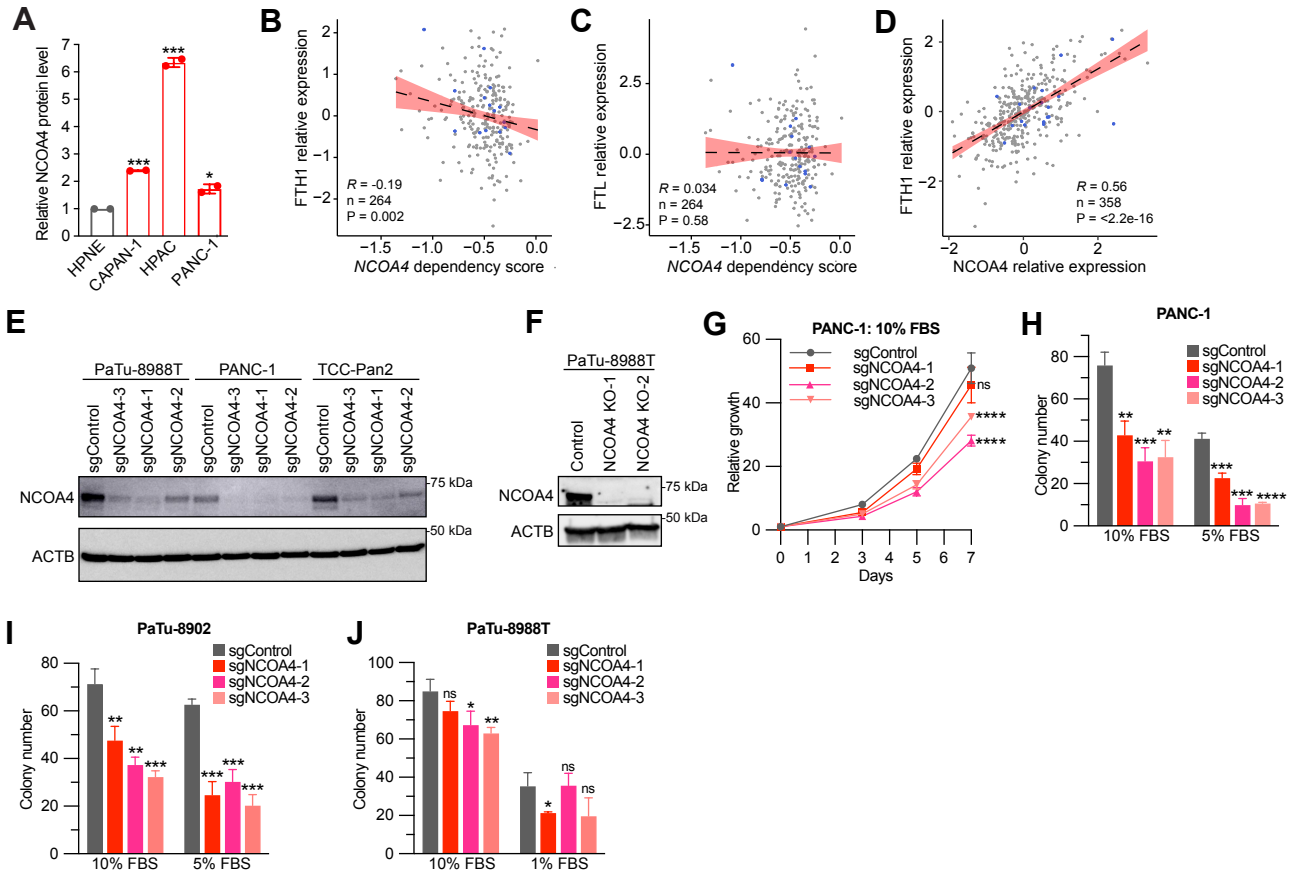

Supplementary Figure S1 NCOA4 is a dependency in PDAC.

A, Relative level of NCOA4 protein as measured by mass spectrometry-based quantitative proteomics of an immortalized human pancreatic ductal epithelial cell line (HPNE) and PDAC cell lines (CAPAN-1, HPAC, PANC-1), data from Paulo et al. 2017 (15). **B,** Scatter plot showing linear regression with 95% confidence interval (black dotted line) and Pearson's correlation coefficient between FTH1 protein expression (y-axis) and *NCOA4* CRISPR dependency scores (x-axis) across 264 cancer cell lines, blue dots represent data for PDAC cell lines. **C,** Scatter plot as in B showing correlation between FTL protein expression (y-axis) and *NCOA4* CRISPR dependency scores (x-axis) across 264 cancer cell lines, blue dots represent data for PDAC cell lines. **D,** Scatter plot showing linear regression with 95% confidence interval (black dotted line) and Pearson's correlation coefficient between FTH1 protein expression (y-axis) and NCOA4 protein expression (x-axis) across 358 cancer cell lines, blue dots represent data for PDAC cell lines. **E,** Immunoblot showing NCOA4 protein levels in lysates from PDAC cell lines lentivirally transduced with control Cas9-sgRNA targeting the non-essential ROSA26 locus (sgControl) or three independent Cas9-sgRNAS targeting *NCOA4* (sgNCOA4-1, -2, -3). **F,** Immunoblot showing NCOA4 protein levels in lysates from control and clonally selected NCOA4 KO PaTu-8988T cell lines. **G,** Relative proliferation of PANC-1 cells lentivirally transduced with sgControl or sgNCOA4-1, -2, or -3 as in E. Data are plotted as relative cell proliferation in arbitrary units. Values normalized to Day 0. Error bars represent s.d. of 6 technical replicates (representative of 3 independent experiments). **H,** Clonogenic growth of PANC-1 cells expressing lentiviral sgRNAs as in G. Left, cells grown in media containing 10% FBS, Right, cells grown in media containing 5% FBS. Error bars ± s.d. triplicate wells of a representative experiment of 3 independent experiments. **I,** Clonogenic growth of PaTu-8902 cells transduced with lentiviral sgControl and sgNCOA4 sgRNAs. Left, cells grown in media containing 10% FBS, Right, cells grown in media containing 5% FBS. Error bars ± s.d. triplicate wells of a representative experiment of 3 independent experiments. **J,** Clonogenic growth of PaTu-8988T cells transduced with lentiviral sgControl and sgNCOA4 sgRNAs. Left, cells grown in media containing 10% FBS, Right, cells grown in media containing 1% FBS. Error bars ± s.d. triplicate wells of a representative experiment of 3 independent experiments. For panels A, G-J, significance determined with *t-test*. ns = $p > 0.05$, * $p < 0.05$, ** $p < 0.01$, *** $p < 0.001$, **** $p < 0.0001$.

Supplementary Figure S2

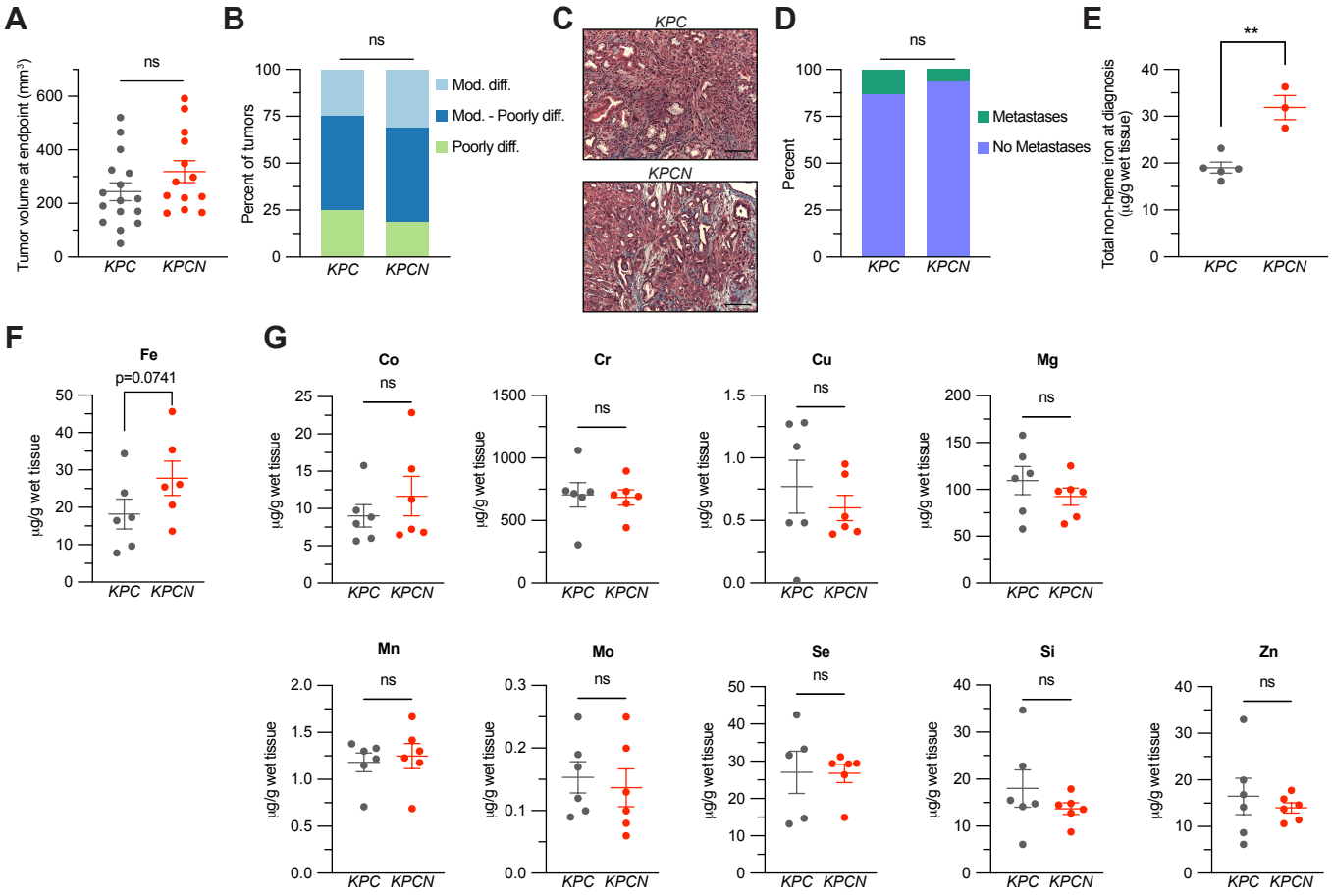

Supplementary Figure S2 Loss of NCOA4 extends murine PDAC survival.
A, Tumor volume at time of endpoint, as measured by ultrasound, *KPC*, n=16, *KPCN*, n=13. **B,** Percentage of *KPC* (n=16) and *KPCN* (n=16) tumors at endpoint classified as moderately differentiated, moderately-poorly differentiated, and poorly differentiated. **C,** Trichrome staining of representative *KPC* and *KPCN* tumors at endpoint. **D,** Percentage of *KPC* (n=15) and *KPCN* (n=16) mice with metastases at endpoint. **E,** Tumor non-heme iron levels in *KPC* versus *KPCN* tumors at diagnosis, n=3-4 tumors per genotype. Significance determined with *t-test*. ** $p < 0.01$. Error bars ± s.e.m. **F,** Tumor total iron (^{56}Fe) at endpoint measured by inductively coupled plasma-mass spectrometry (ICP-MS), n=6 tumors per genotype, one-tail *t test*. **G,** ICP-MS of Co, Cr, Cu, Mg, Mn, Mo, Se, Si, Zn levels in *KPC* versus *KPCN* tumors at endpoint, n=6 tumors per genotype. Error bars ± s.e.m.

Supplementary Figure S3

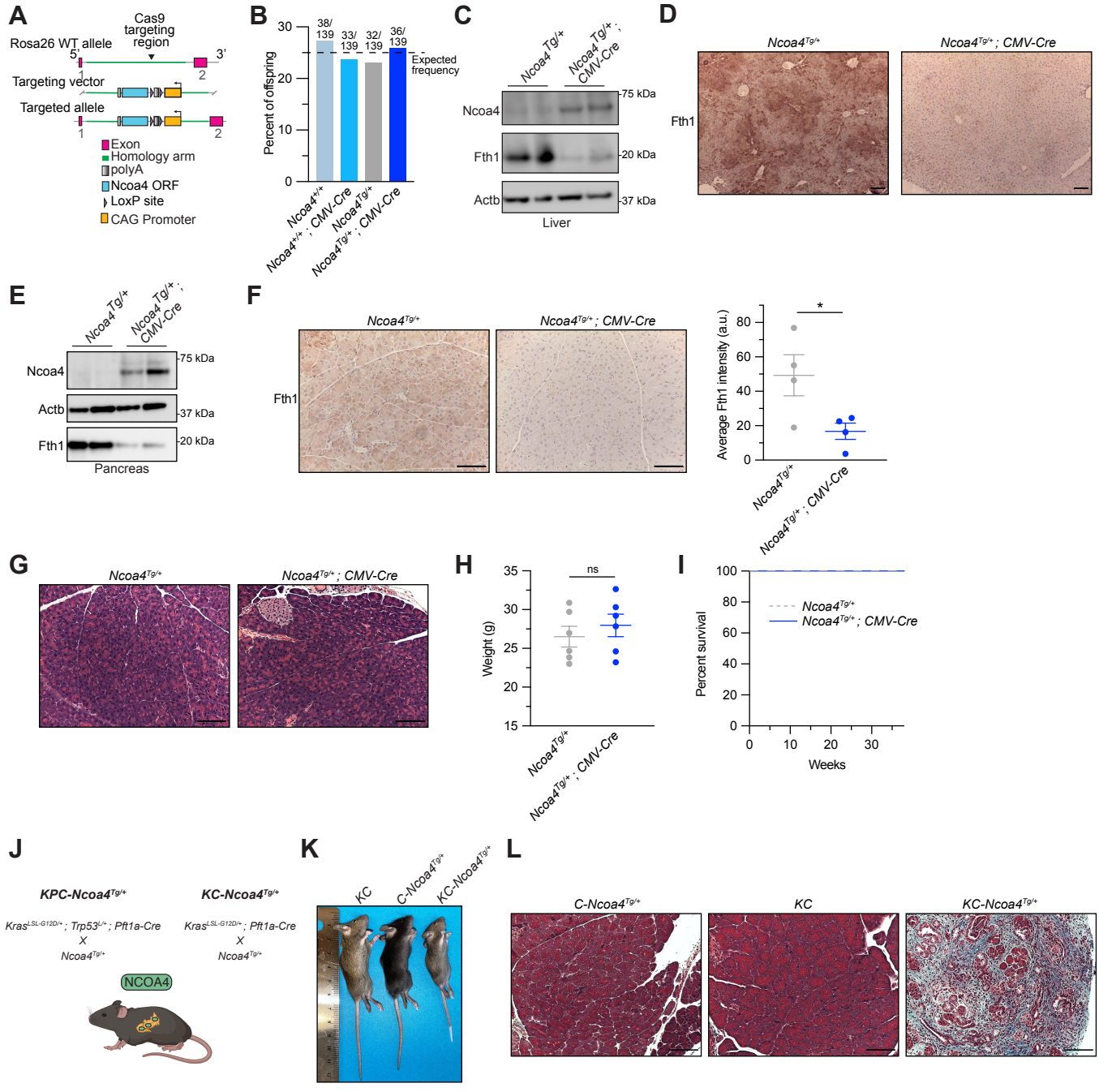

Supplementary Figure S3 NCOA4 overexpression accelerates ferritinophagy *in vivo*.

A, Schematic of construction of a conditional *Ncoa4*$^{Tg/+}$ overexpression allele using Cas9-mediated knock-in of a *Ncoa4* ORF at the *Rosa26* locus with upstream loxP sites. **B,** Genotype frequency of *Ncoa4*$^{+/+}$, *Ncoa4*$^{+/+}$; *CMV-Cre, Ncoa4*$^{Tg/+}$, and *Ncoa4*$^{Tg/+}$; *CMV-Cre* mice among 139 genotyped offspring mice, dotted line represents expected frequency of genotypes (25%). **C,** Immunoblot showing Ncoa4 and Fth1 protein levels in lysates from livers harvested from *Ncoa4*$^{Tg/+}$ and *Ncoa4*$^{Tg/+}$; *CMV-Cre* mice. **D,** Fth1 immunostaining from livers harvested from *Ncoa4*$^{Tg/+}$ and *Ncoa4*$^{Tg/+}$; *CMV-Cre* mice, representative image, Scale bar = 50 μm. **E,** Immunoblot showing Ncoa4 and Fth1 protein levels in lysates from pancreata harvested from *Ncoa4*$^{Tg/+}$ and *Ncoa4*$^{Tg/+}$; *CMV-Cre* mice. **F,** Fth1 immunostaining from pancreata harvested from *Ncoa4*$^{Tg/+}$ and *Ncoa4*$^{Tg/+}$; *CMV-Cre* mice, representative image, Scale bar = 50 μm. Quantification of average Fth1 intensity in arbitrary units (5 random fields per sample, n=4 mice/group, error bars represent ±s.e.m.). **G,** H&E staining of pancreata harvested from *Ncoa4*$^{Tg/+}$ and *Ncoa4*$^{Tg/+}$; *CMV-Cre* mice, representative image. **H,** Body weight of *Ncoa4*$^{Tg/+}$ mice versus *Ncoa4*$^{Tg/+}$; *CMV-Cre* mice measured at 38 weeks of age, n=6 animals per genotype. **I,** Kaplan-Meier analysis comparing overall survival of *Ncoa4*$^{Tg/+}$ (n=6) mice versus *Ncoa4*$^{Tg/+}$; *CMV-Cre* (n=6) mice. **J,** Schematic of generation of *KC-Ncoa4*$^{Tg/+}$ and *KPC-Ncoa4*$^{Tg/+}$ mice. **K,** Picture of representative *KC*, *C-Ncoa4*$^{Tg/+}$, and *KC-Ncoa4*$^{Tg/+}$ mouse at 3 weeks of age demonstrating decreased size of *KC-Ncoa4*$^{Tg/+}$ mouse. **L,** Trichrome staining of representative pancreata from 3-week-old *C-Ncoa4*$^{Tg/+}$, *KC*, and *KC-Ncoa4*$^{Tg/+}$ mice. Scale bar = 50 μm. For panels F and H significance determined with *t test*. ns = not significant: $p > 0.05$, * $p < 0.05$. Error bars ± s.e.m.

Supplementary Figure S4

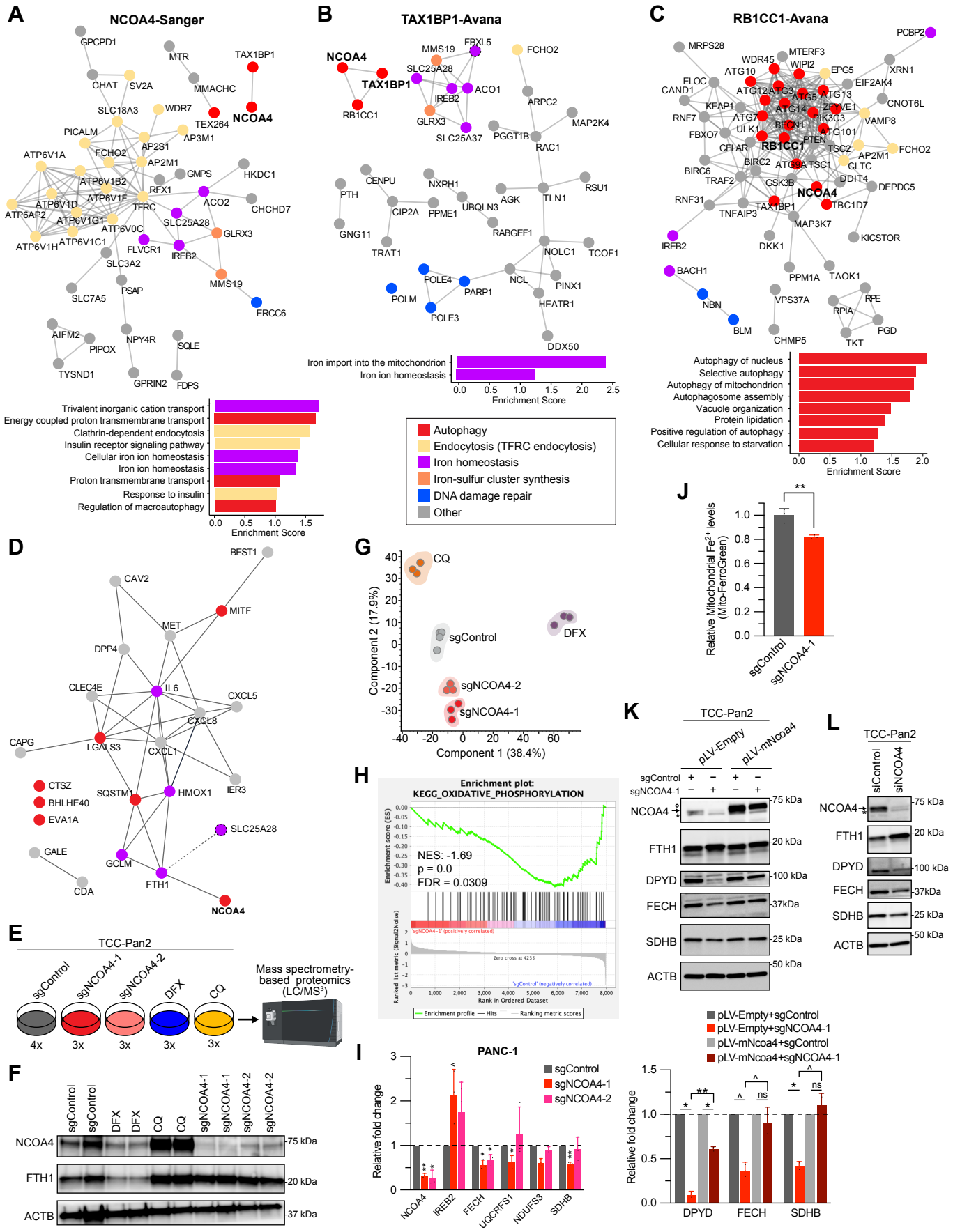

Supplementary Figure S4 NCOA4, TAX1BP1, and RB1CC1 dependencies are correlated with iron metabolism genes.

A, Network map showing gene dependencies most highly correlated with *NCOA4* dependency in the Sanger Cancer Dependency Map. Grey connections indicate interaction between genes as predicted by STRING. Gene Ontology Biological Process (GO BP) enrichment analysis, depicted below. Coloring of genes is as noted in the box based on GO BP enrichment. **B,** Network map showing gene dependencies most highly correlated with *TAX1BP1* dependency in the Cancer Dependency Map (21Q1). Grey connections indicate interaction between genes as predicted by STRING. Gene Ontology Biological Process enrichment analysis, depicted below. Coloring of genes is as noted in the box based on GO BP enrichment. *FBXL5* is denoted by a hashed circle as it is anti-correlated to *TAX1BP1* dependency. **C,** Network map showing gene dependencies most highly correlated with *RB1CC1* dependency in the Cancer Dependency Map (21Q1), as in B. **D,** Network of genes whose mRNA expression level are most highly anti-correlated with *NCOA4* dependency across 772 cancer cell lines. *SLC25A28* is denoted by a hashed circle as it is positively correlated to *NCOA4* dependency. Grey connections indicate interaction between genes as predicted by STRING, coloring of gene nodes is as noted in the box. **E,** Schematic of 16 sample multiplexed proteome experiment from TCC-Pan2 cells treated as indicated. **F,** Immunoblot showing NCOA4 and FTH1 protein levels in lysates from TCC-Pan2 cells lentivirally transduced with sgControl, sgNCOA4-1, sgNCOA4-2, or sgControl also treated with DFX (30 μM, 16 hours) or CQ (10 μM, 16 hours). Two representative lysates shown from samples prepared for proteome experiment as depicted in E. **G,** Principal component analysis of the TCC-Pan2 sgControl, sgNCOA4-1, sgNCOA4-2, DFX, and CQ proteomes represented in a two-dimensional space. **H,** Enrichment plot for Gene Ontology (Molecular Function) Metal Cluster Binding gene set of sgNCOA4-1 compared to sgControl TCC-Pan2 proteome, oxidative phosphorylation is negatively enriched in sgNCOA4-1 compared to sgControl proteome. **I,** Relative fold-change quantification of PANC-1 results displayed in Figure 4G and is of 2-3 replicates. Significance determined with *t-test*. * $p < 0.05$, ** $p < 0.01$. Error bars are ± s.d. **J,** Quantification of mitochondrial Fe^{2+} by Mito-FerroGreen staining and flow cytometry in TCC-Pan2 *NCOA4* KD cells. Mean fluorescence intensity was normalized to cells transduced with sgControl. Error bars ± s.d. of 3 independent measurements. **K,** Immunoblot showing ISC protein levels in lysates from TCC-Pan2 cell lines lentivirally transduced with pLV-Empty vector control or pLV-mNcoa4 encoding a 3xFLAG-mNcoa4 (murine Ncoa4) sgNCOA4-1 resistant construct and either sgControl or sgNCOA4-1, as indicated. Relative fold-change quantification is of two replicates. NCOA4 blot: the open circle denotes exogenous pLV-3x-FLAG-mNcoa4, the arrow denotes endogenous NCOA4, and the asterisk denotes a contaminant. **L,** Immunoblot showing ISC protein levels in lysates from TCC-Pan2 cell lines transfected with siRNA targeting NCOA4 (siNCOA4) or non-targeting control (siControl). The arrow denotes endogenous NCOA4, and the asterisk denotes a contaminant. For panels I-K, significance determined with *t-test*. ns = non-significant: $p>0.1$, ^ $p<0.1$, * $p < 0.05$, ** $p < 0.01$. Error bars are ± s.d.

Supplementary Figure S5

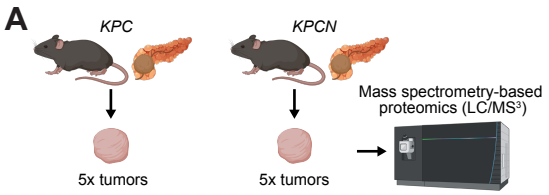

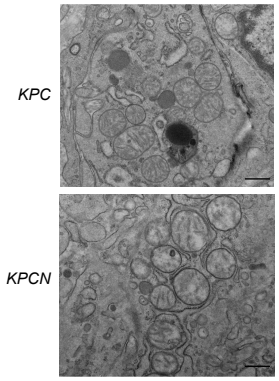

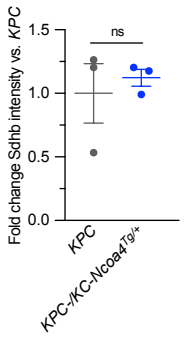

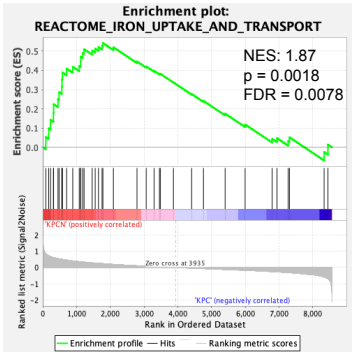

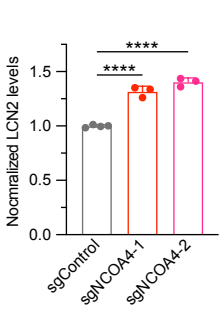

Supplementary Figure S5 Ncoa4 ablation in PDAC tumors leads to compensatory iron acquisition pathways.

A, Schematic of 10-sample multiplexed proteome experiment of *KPC* versus *KPCN* tumors (n=5 tumors per genotype). **B,** Representative electron micrographs of mitochondria from *KPC* and *KPCN* tumors as quantified in Figure 5E. Scale bar, 500 nm. **C,** Quantification of Sdhb immunostaining of tumors from *KPC* and *KPC-Ncoa4*$^{Tg/+}$ */ KC-Ncoa4*$^{Tg/+}$ mice. Relative fold change to *KPC* tumors presented (5 random fields per tumor, n=3 mice/group, error bars represent ± s.e.m.). **D,** Enrichment plot for Reactome Iron uptake and transport gene set of *KPCN* compared to *KPC* tumor proteomes. **E,** Relative protein levels of LCN2 as measured in global TCC-Pan2 sgControl (n=4), sgNCOA4-1 (n=3) and sgNCOA4-2 (n=3) proteomes, normalized to sgControl levels (error bars represent s.d.). For panels C, E significance determined with *t test*. ns = not significant, $p > 0.05$, ****$p<0.0001$.

Supplementary Figure S6

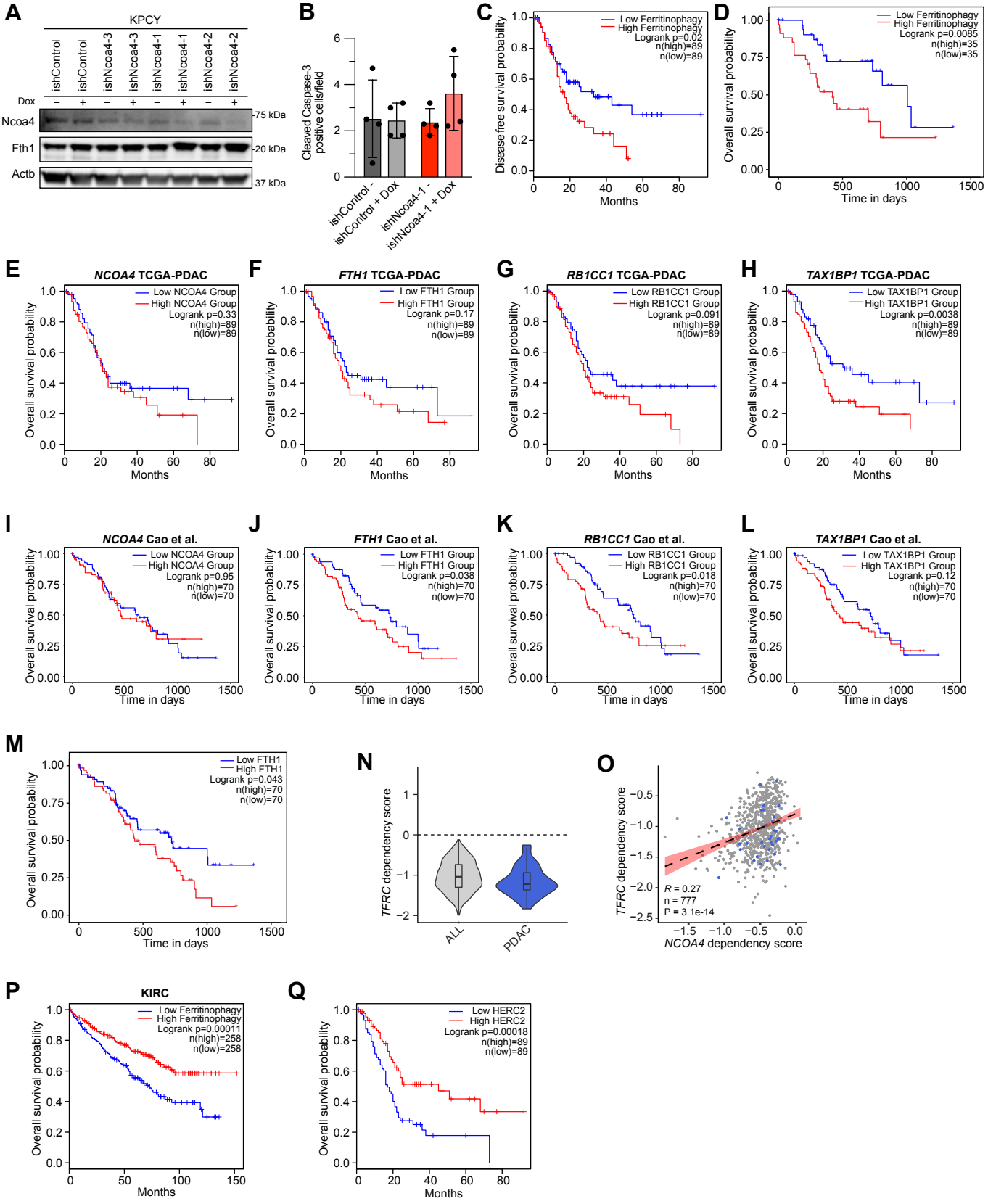

Supplementary Figure S6 NCOA4-mediated ferritinophagy expression signature is a prognostic marker in human PDAC.

A, Immunoblot showing Ncoa4 and Fth1 protein levels in lysates from KPCY cells expressing ishControl, ishNCOA4-1, ishNCOA4-2, and ishNCOA4-3 and treated with or without doxycycline (100 ng/mL, 3 days), as indicated. **B,** Quantification of Cleaved Caspase-3 immunohistochemistry from *in vivo* subcutaneous tumors in C57BL/6 mice of KPCY ishControl versus ishNcoa4-1 cells with and without doxycycline containing food (as in Fig. 6B-C). Number of Cleaved Caspase-3 positive cells was counted in 5 fields from each tumor, n=4 tumors per group. All comparisons non-significant. **C,** Disease-free survival analysis with log-rank test of a Ferritinophagy gene expression signature (*NCOA4, FTH1, TAX1BP1, RB1CC1*) in PDAC using TCGA dataset. **D,** Survival analysis with log-rank test of a Ferritinophagy gene expression signature (*NCOA4, FTH1, TAX1BP1, RB1CC1*) in PDAC using Cao et al. 2021 (37) dataset using 25^{th} and 75^{th} percentile cutoffs for ferritinophagy signature. **E-H**, Survival analysis with log-rank test of individual *NCOA4, FTH1, RB1CC1, and TAX1BP1* gene expression in PDAC using TCGA dataset. **I-L,** Survival analysis with log-rank test of individual *NCOA4, FTH1, RB1CC1, and TAX1BP1* gene expression in PDAC using Cao et al. 2021 dataset (37). **M,** Survival analysis with log-rank test of FTH1 protein level in PDAC as measured by mass spectrometry-based proteomics in Cao et al. 2021 (37). **N,** Violin plot of CRISPR dependency scores of *TFRC* in all cancer cell lines represented in Dependency Map (n=789) and PDAC cell lines (n=34), Box = quartile ranges and line = median value. **O,** Scatter plot showing linear regression with 95% confidence interval (black dotted line) and Pearson's correlation coefficient between *TFRC* CRISPR dependency scores (y-axis) and *NCOA4* CRISPR dependency scores (x-axis) across 777 cancer cell lines, blue dots represent data for PDAC cell lines. **P,** Survival analysis with log-rank test of a Ferritinophagy gene expression signature (*NCOA4, FTH1, TAX1BP1, RB1CC1*) in Kidney Renal Clear Cell Carcinoma (KIRC) using the TCGA dataset. **Q,** Survival analysis with log-rank test of *HERC2* gene expression in PDAC using the TCGA dataset.

SUPPLEMENTARY TABLES

Supplementary Table 1 TCC-Pan2 proteome, *KPCN* versus *KPC* proteome

Supplementary Table 2 TCC-Pan2, *KPCN* GSEA

Supplementary Table 3 Cancer Therapeutics Response Portal NCOA4 correlations